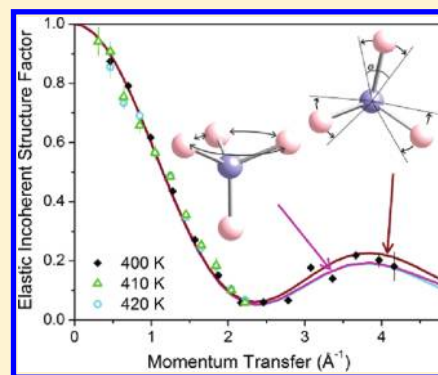


The Nature of BH_4^- Reorientations in Hexagonal LiBH_4

Nina Verdal,^{*,†} Terrence J. Udovic,[†] and John J. Rush^{†,‡}[†]NIST Center for Neutron Research, National Institute of Standards and Technology, 100 Bureau Dr., MS 6102, Gaithersburg, Maryland 20899-6102, United States[‡]Department of Materials Science and Engineering, University of Maryland, 2135 Chemical & Nuclear Engineering Bldg., College Park, Maryland 20742-2115, United States**S** Supporting Information

ABSTRACT: Lithium borohydride (LiBH_4) has lately been the subject of intense inquiry within the hydrogen storage community. Quasi-elastic neutron scattering spectra were measured for LiBH_4 in the high-temperature hexagonal crystal phase. The elastic incoherent structure factor associated with the rapid BH_4^- anion reorientations was determined at 400, 410, and 420 K for momentum transfers as high as 4.2 \AA^{-1} . The results strongly suggest a BH_4^- reorientational mechanism approaching quasi-free, trigonal-axis rotation of three borohydride H atoms, combined with reorientational jump exchanges between these delocalized “orbiting” H atoms and the remaining axial borohydride H atom. This mechanism is consistent with previously reported diffraction and spectroscopy studies.



INTRODUCTION

Lithium borohydride (LiBH_4) has been the subject of much investigation in recent years as a potential hydrogen storage material for mobile applications, due in part to its inherently large gravimetric and volumetric hydrogen density. The structure and vibrational dynamics of this material have been studied extensively. LiBH_4 undergoes a phase transition¹ around 380 K from an orthorhombic ($Pnma$) to a hexagonal ($P6_3mc$) structure (Figure 1a). A heat capacity study² reported an entropy change of $16.65 \text{ J}/(\text{mol K})$ for the phase transition, a magnitude suggestive of the presence of BH_4^- disorder in hexagonal LiBH_4 . Crystallographic studies^{3,4} have indicated that the H thermal ellipsoids of the BH_4^- group in the hexagonal phase are very large even at 400 K but can be described as localized. One synchrotron X-ray diffraction (XRD) study³ interpreted the H thermal ellipsoids to be large enough so as to be “nearly isotropic” and attributed this to a substantial “libration-like” component to the electron density. According to a LiBD_4 neutron powder diffraction (NPD) study,⁴ the BD_4^- anions are “extremely disordered”. An earlier synchrotron XRD study⁵ described the hexagonal phase as having “dynamic disorder about the BH_4^- trigonal axis”. Additionally, computational studies had asserted that the stability of the $P6_3mc$ crystal structure relies on the presence of dynamical disorder.⁶ A Raman spectroscopy study⁷ reported an increase of line widths above the phase-transition temperature attributable to “large-amplitude librational motions of quasi-rigid BH_4^- tetrahedra about their trigonal axis”. An analysis of neutron vibrational spectra⁸ showed a low-energy phonon density of states characteristic of glassy and disordered systems. First-principles molecular dynamics simulations⁹

have predicted hydrogen density nearly spherically distributed about the boron atom.

The reorientational dynamics of the BH_4^- anion in the hexagonal phase has seen much more limited investigation.^{10–13} Yet, a proper description of these dynamics is key to understanding the nature of the BH_4^- disorder and the role it plays in the stability of LiBH_4 polymorphs.^{3,14} Quasi-elastic neutron scattering (QENS) is uniquely capable of determining the geometric details of the BH_4^- reorientational mechanism. A recent QENS study of the hexagonal LiBH_4 phase¹¹ suggested a BH_4^- reorientational mechanism akin to that observed for the other disordered cubic alkali-metal borohydrides, namely, 90° jump rotations about the three molecular C_2 -axes of the tetrahedral anions. In effect, this can be described as an anion tumbling motion such that, over time, the H atoms visit the eight corners of a cube, resulting in BH_4^- crystallographic disorder. Although the QENS data were in fair agreement with such a mechanism, the required cubic disorder is inconsistent with the observed hexagonal structure. Moreover, since the measurements were restricted to momentum transfers (Q) $< 2.6 \text{ \AA}^{-1}$, they were unable to test the cubic tumbling mechanism at higher Q values where the QENS measurements are more mechanism-dependent. In the current paper, we present QENS results for hexagonal LiBH_4 over a more extensive Q range. These results are found to be in disagreement with the previously proposed cubic tumbling mechanism. Rather, they strongly suggest an alternate reorientational mechanism that is consistent with prior diffraction and spectroscopy results.

Received: December 6, 2011

Published: December 12, 2011

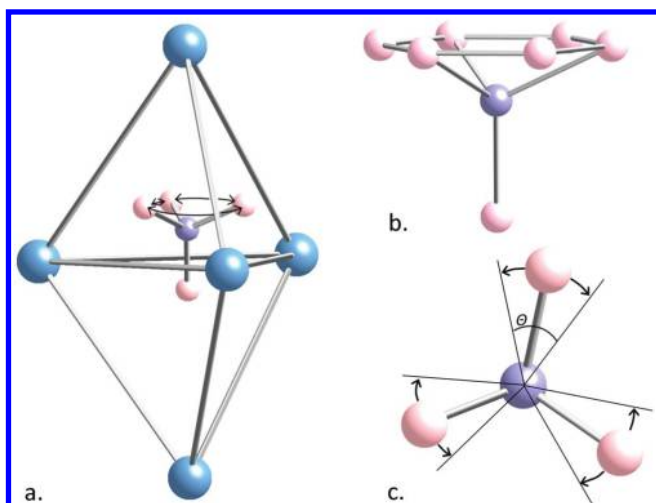


Figure 1. (a) Local structural arrangement of hexagonal LiBH_4 . The arrows indicate the reorientational motion about the trigonal C_3 -axis. (b) Schematic of the high-temperature model described in eq 6 for $N = 6$. (c) View along the c -axis depicting the partial delocalization model of the trigonal H atoms subtending an angle θ . The spheres shown here represent hydrogen (pink), lithium (blue), and boron (purple) atoms.

Neutron scattering methods are well-suited to probing H atoms because the incoherent scattering cross section for hydrogen is an order of magnitude greater than that of other atoms. QENS can probe H motions that occur on the order of nanoseconds to picoseconds, as a function of neutron energy transfer ($\hbar\omega$) and momentum transfer, depending on instrument capabilities and configurations. In the case of covalently bound H atoms in a crystal lattice, these motions commonly involve occasional rotational jumps over a barrier on the potential energy surface to a different, but crystallographically equivalent, molecular configuration. QENS spectra consist of an elastic line $\delta(\omega)$ and a broader quasi-elastic feature, in practice convolved by the instrument resolution function. In the present case, the quasi-elastic feature is the manifestation of a neutron peak broadening due to energy exchange of the neutron with the reorienting BH_4^- anions. It is generally represented by one or more Lorentzian functions, $L_i(\omega)$, centered at the elastic line. The scattering function then becomes

$$S(Q, \omega) = A_0(Q)\delta(\omega) + \sum A_i(Q)L_i(\omega) \quad (1)$$

The ratio of the elastic peak area $A_0(Q)$ to the total scattering area ($A_0(Q) + \sum A_i(Q)$) is known as the elastic incoherent structure factor (EISF). Careful interpretation of the EISF as a function of momentum transfer can reveal the mechanism and geometry of the observed dynamics.

EXPERIMENTAL METHODS

${}^7\text{Li}^{11}\text{BH}_4$ was purchased from Katchem¹⁵ with >95% purity and 99.8% isotopic enrichment of both ${}^7\text{Li}$ and ${}^{11}\text{B}$. The exclusion of ${}^6\text{Li}$ and ${}^{10}\text{B}$ isotopes increases the neutron transmission considerably since they are both very strong neutron absorbers. All neutron scattering measurements were performed at the NIST Center for Neutron Research. QENS measurements were collected on the disk chopper spectrometer¹⁶ (DCS) with incident neutron wavelengths of 2.75 Å (10.8 meV incident neutron energy, elastic line 275 μeV fwhm) at 400 K and 5 Å (3.3 meV

incident neutron energy, elastic line 105 μeV fwhm) at 410 and 420 K. In addition, for each incident neutron energy, resolution functions were measured with the sample at 135 K. The QENS spectra were reduced and analyzed using the DAVE¹⁷ software package.

RESULTS AND DISCUSSION

In agreement with a previous study,¹¹ the quasi-elastic scattering intensity associated with each QENS measurement in the current study was found to be well-represented by a single Lorentzian function. Therefore, each spectrum was fit to a Lorentzian function, delta function, and linear baseline, convolved with an instrument resolution function. The resulting quasi-elastic line widths (~ 3 meV fwhm) at 400, 410, and 420 were in good agreement with those reported in a previous QENS study¹¹ at lower momentum transfers. In that study, quasi-elastic line widths were measured over a broader temperature range between 400 and 590 K and fit to an Arrhenius equation, yielding an activation energy of 6.6 ± 0.5 kJ/mol,¹¹ indicative of a low barrier to reorientation (i.e., a rather shallow H potential well around the rotation coordinate). The focus of the present work was not to repeat the temperature-dependent measurements performed previously. Rather, our goal was to assess the mechanism for BH_4^- reorientations in the high-temperature hexagonal phase of LiBH_4 by determining the EISF over a more extensive Q range and compare it with the previously proposed^{11,18} cubic tumbling model.

Proper interpretation of our EISFs assumes that we are capturing all of the quasi-elastic scattering intensity from BH_4^- reorientational motions in the broad component of our spectra and are able to completely separate out the purely elastic scattering. It should be noted that our EISFs do not depend on having to more rigorously model the quasi-elastic peak shape with multiple Lorentzians. Only the integrated quasi-elastic scattering intensity is required, which we and others^{11,18} show is adequately determined by a single Lorentzian. Since we used elastic peak resolutions of 105 and 275 μeV , we were sensitive to potential Lorentzian components on the order of 10 and 30 μeV wide, respectively, which are over 2 orders of magnitude less than the observed quasi-elastic broadening. Nonetheless, we see nothing else that broadens the elastic peak further beyond that from the low-temperature resolution function measurement. If there were an even narrower quasi-elastic component buried under the elastic peak, we are confident, based on all of our prior experience with studying dynamics in borohydrides, that it would not be due to BH_4^- reorientational motions. In the current study, the EISFs at 410 and 420 K contain data points for momentum transfers up to 2.2 Å⁻¹. Within this limited Q range, they agree with the data collected at 400 K, which contains points in momentum transfer out to 4.2 Å⁻¹. We therefore assume that the same reorientation mechanism dominates over the temperature range of at least 400–420 K. The observed EISFs were compared to a number of reorientation models, shown in Figure 2. For each model, we assume that the BH_4^- anion in hexagonal LiBH_4 is a perfect tetrahedron with a B–H bond length of 1.14 Å. These models are described below.

If the BH_4^- anion is jump reorienting about all four tetrahedral C_3 -axes (i.e., in effect, tumbling among tetrahedral H sites), the EISF would behave according to¹⁹

$$\text{EISF}_{\text{tetrahedral}} = \frac{1}{4}(1 + 3j_0(Qr\sqrt{3})) \quad (2)$$

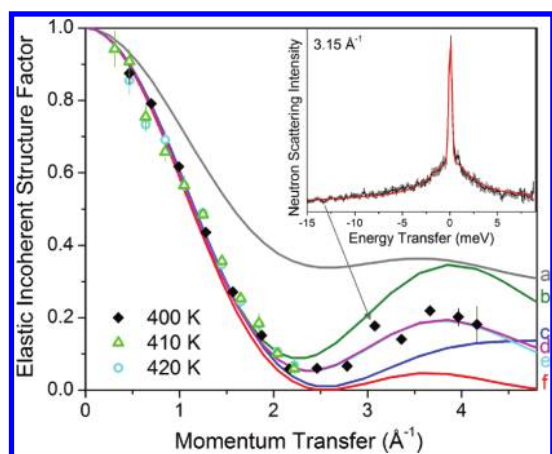


Figure 2. EISF data derived from QENS measurements for LiBH_4 at 400 K (black diamonds), 410 K (green triangles), and 420 K (cyan circles) compared with calculated curves for various reorientation models: (a) continuous rotation around the trigonal axis with a fixed axial H (gray), (b) tetrahedral tumbling (green), (c) cubic tumbling (blue), (d) the high-temperature model for $N = 6$ (magenta), (e) the high-temperature model for $N \geq 12$ (cyan), and (f) isotropic rotational diffusion (red). The inset exemplifies a quasi-elastic spectrum (black data), collected at 400 K at 3.15 \AA^{-1} , and the corresponding fit (red line). Vertical error bars denote $\pm 1\sigma$.

in which j_0 is the zeroth-order spherical Bessel function, r is the B–H bond length, and $r\sqrt{3}$ is the distance between two H atoms. This model is represented by the green line (b) in Figure 2. Crystallographically, this dynamic is consistent with an ordered structure and full occupancy in the tetrahedral H positions.

The cubic tumbling model, as proposed previously,¹¹ involves tetrahedra with reorientational disorder. A 90° jump about a C_2 -axis moves an H atom from one corner of a cube to an adjacent one, retaining cubic symmetry but inducing disorder from tetrahedral symmetry, each H position possessing half-occupancy. The EISF behaves according to²⁰

$$\text{EISF}_{\text{cubic}} = 1 + 3j_0(Qa) + 3j_0(Qa\sqrt{2}) + j_0(Qa\sqrt{3}) \quad (3)$$

in which $a = 2r/\sqrt{3}$ is the jump distance, equivalent to one side of the cube. This model is represented by the blue line (c) in Figure 2. It is a good representation of the dynamics observed in the high-temperature, cubic phases of KBH_4 and NaBH_4 .²¹ As mentioned earlier, it is, however, a problematic mechanism for the high-temperature phase of LiBH_4 since it violates hexagonal crystal symmetry.

In the case in which the BH_4^- H atoms are not making discrete jumps to crystallographically equivalent configurations, but are making random jumps on the surface of a sphere with a radius equal to the B–H bond length r such that, over time, the H atoms visit the entire surface of the sphere, the observed EISF would follow the model for isotropic rotational diffusion:^{22,23}

$$\text{EISF}_{\text{iso}} = j_0^2(Qr) \quad (4)$$

This model describes isotropic rotational disorder and would be consistent with crystallographic data that showed the boron completely surrounded by a spherical shell of hydrogen

scattering density. This model is represented by the red line (f) in Figure 2.

Even though the thermal ellipsoids as interpreted from high-temperature synchrotron XRD data³ indicate “nearly isotropic disorder” of the borohydride, the present QENS data, which were collected over an extended, more model-sensitive Q range, clearly do not agree with an isotropic reorientational diffusion model (eq 4) or, for that matter, the tetrahedral (eq 2) or cubic tumbling (eq 3) models proposed thus far. Hence, after discounting these models as likely candidates, we sought instead to develop an alternate model for reorientation that was consistent with the space group and extended thermal ellipsoids derived in previous crystallographic studies.^{3,4} In what follows, we show that such a reorientation model exists which is in very good agreement with the observed data up to momentum transfers of 4.2 \AA^{-1} .

The proposed model was developed from the observation from the earlier synchrotron XRD study⁵ that the BH_4^- anion displays dynamical disorder only around its trigonal (c -parallel) C_3 -axis. A similar conceptual model, also inspired by the synchrotron study, was suggested to describe previous Raman spectroscopy results.²⁴ Hence, we postulated that three H atoms of the BH_4^- anion occupy N equally spaced points on a circle (at $3/N$ occupancy, where $N = 3l$; $l = 2, 3, 4, \dots$), jumping $2\pi/N$ radians about the trigonal axis (e.g., for $N = 6$; see Figure 1b), possibly approaching quasi-free reorientational motion. In addition, any of these three orbiting H atoms can exchange positions with the remaining axial H atom via appropriate C_2 -axis and/or C_3 -axis reorientations. For large enough N (12 in this case), the small jumps about the trigonal axis approximate continuous rotation.^{22,23,25,26}

The EISF for N jumps about a circle of radius r is written^{22,25}

$$\text{EISF}_{C_N} = \frac{1}{N} \sum_{p=1}^N j_0 \left(2Qr \left[\sin \frac{\pi p}{N} \right] \right) \quad (5)$$

This is incorporated into our “high-temperature” model, following the methodology presented in ref 26, in which three-quarters of the H atoms participate in the jumps about a circle and one-quarter of the H atoms occupy the axial position. The generalized EISF for this model is

$$\text{EISF}_{\text{HT}} = \frac{1}{\frac{N}{3} + N} \left\{ \frac{1}{4} \left[\frac{N}{3} + N j_0(Qr\sqrt{3}) \right] + \frac{3}{4} \left[\frac{N}{3} j_0(Qr\sqrt{3}) + \sum_{p=1}^N j_0 \left(2Qr \left[\sin \frac{\pi p}{N} \right] \right) \right] \right\} \quad (6)$$

in which $r\sqrt{3}$ is the distance between the axial hydrogen and a hydrogen atom on the circle. This model is illustrated in Figure 2 for $N = 6$ and $N \geq 12$ (the latter sufficiently approximating one-dimensional rotational diffusion over the measured Q range) by the magenta (d) and cyan (e) lines, respectively.

It is evident that the QENS data are in very good agreement with this “high-temperature” model (eq 6) for $N \geq 6$. The predicted EISFs are indistinguishable in the collected Q range for $N \geq 6$, but at an even higher Q range, the EISFs for $N = 6$ (6-fold jumps) and $N \geq 12$ (approximating continuous rotation) diverge. It is uncertain to what extent diffraction can help distinguish between three or six discrete H positions about a circle or even something more diffuse, given the large thermal ellipsoids evident from previous diffraction analyses. Nonetheless,

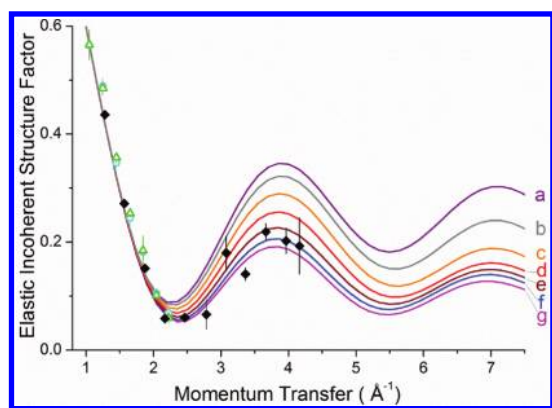


Figure 3. EISF data derived from QENS measurements collected at 400 K (diamonds), 410 K (triangles), and 420 K (circles) compared with calculated curves from the partial-delocalization reorientation model described in the text, for θ values of (a) 0° (purple), (b) 15° (gray), (c) 30° (orange), (d) 45° (red), (e) 60° (brown), (f) 75° (blue), and (g) 120° (magenta). Vertical error bars denote $\pm 1\sigma$.

it is clear that any model capable of reproducing the data must assume a more diffuse distribution of H atoms around the trigonal axis than $N = 3$, which is consistent with the nearly isotropic disorder suggested by diffraction and spectroscopy measurements. Within the Q range measured, we can conclude that the H atoms rotating about the molecular C_3 -axis are undertaking reorientational steps about a circle, approaching quasi-free rotation. It is important to emphasize that for $N = 3$, eq 6 simplifies to eq 2, the tetrahedral tumbling model, which is clearly inconsistent with the QENS data. We also point out that exchanges between axial and trigonal H atoms are an additional critical aspect of the observed mechanism. Indeed, if we alter eq 5 (see the Supporting Information for details) to include a purely elastic scattering contribution from a “stationary” axial H atom, the resulting modified EISF (see the gray line (a) in Figure 2) is also inconsistent with the QENS data.

An additional attempt was made to develop a modified disordered model that reflected the fairly shallow rotational potentials⁸ and broad thermal ellipsoids observed around the rotational coordinate of the trigonal axis. In other words, instead of assuming either full localization at their crystallographic positions or full delocalization around their trigonal axis, we allowed the three trigonal H atoms to be partially delocalized around their rotational circle within $\pm(\theta/2)$ radians of their crystallographic positions, thus leaving angular gaps of $2\pi/3 - \theta$ radians between the three H-occupied angular regions (see Figure 1c). Hence, we created a modified version of eq 6 for large N in which these angular gaps in H atom occupation were excluded from the list of allowable jump locations (see the Supporting Information for details). In the lower limit of $\theta = 0$, the three H atoms are fully localized in their crystallographic positions, and the EISF is identical to the tetrahedral tumbling model (eq 2). In the upper limit of $\theta = 2\pi/3$ (120°), there are no angular gaps, three atoms are fully delocalized around the trigonal axis, and the EISF is identical to the high-temperature model (eq 6). Figure 3 depicts the QENS data compared with the EISFs resulting from various values of θ between 0 and $2\pi/3$. There is agreement between data and the calculation for $\theta \geq 2\pi/6$ (60°). It is interesting to note that a cluster of hydrogen density subtending 60° is of the order of the width of the thermal ellipsoids reported from NPD.⁴

We have been able to develop reasonable reorientational models to fit the QENS data. No effort was made to develop a more detailed analysis of the quasi-elastic peak shape to compare the relative dynamics of the three H atoms within the delocalized circle to the coupled jump exchanges with the remaining axial H atom. A single Lorentzian was found to be sufficient to accurately capture the intensity of the quasi-elastic portion of the total scattering and thus allowed us to determine the EISF. In reality, within this quasi-elastic envelope, there are a combination of line widths due to the reorientational motions of the three H atoms around the trigonal C_3 -axis and the jumps involving the axial H atom around other C_2 - and/or C_3 -axes. There would likely be a distribution of jump barriers involving the axial H atom, since the barrier for any axial H atom jump will depend on the locations of the other three trigonal H atoms at the time of the jump. It is unlikely that such a detailed investigation of the quasi-elastic peakshape would be conclusive or improve our understanding of the system.

CONCLUSION

Quasi-elastic neutron scattering spectra have been collected for the high-temperature hexagonal phase of LiBH_4 at 400, 410, and 420 K. Data were collected at 400 K for momentum transfers out to 4.2 \AA^{-1} , such a high Q value being crucial for probing the BH_4^- reorientational mechanism in this crystal lattice. The observed EISFs were compared with various possible models for reorientation. Our QENS results strongly suggest a reorientational mechanism described by either partial or full delocalization of the three H atoms around the trigonal axis coupled with jump exchanges with the remaining axial H atom. The data place a lower limit of around 60° for H atom delocalization around the trigonal axis. These findings contradict a previous QENS analysis but are in agreement with other experimental and calculational studies.

ASSOCIATED CONTENT

S Supporting Information. Derivation of EISFs referred to in the paper. This material is available free of charge via the Internet at <http://pubs.acs.org>.

AUTHOR INFORMATION

Corresponding Author

*E-mail: Nina.Verdal@nist.gov.

ACKNOWLEDGMENT

This work utilized facilities supported in part by the National Science Foundation under Agreement DMR-0944772. This work was partially supported by the DOE through EERE Grant DE-EE0002978.

REFERENCES

- (1) Gorbunov, V. E.; Gavrichev, K. S.; Zalukaev, V. L.; Sharpataya, G. A.; Bakum, S. I. *Russ. J. Inorg. Chem.* **1984**, *29*, 1334.
- (2) Gavrichev, K. S. *Inorg. Mater.* **2003**, *39*, S89.
- (3) Filinchuk, Y.; Chernyshov, D.; Cerny, R. *J. Phys. Chem. C* **2008**, *112*, 10579.
- (4) Hartman, M. R.; Rush, J. J.; Udovic, T. J.; Bowman, R. C., Jr.; Hwang, S.-J. *J. Solid State Chem.* **2007**, *180*, 1298.

- (5) Soulié, J.-P.; Renaudin, G.; Černý, R.; Yvon, K. *J. Alloys Compd.* **2002**, *346*, 200.
- (6) Łodziana, Z.; Vegge, T. *Phys. Rev. Lett.* **2006**, *97*, 119602.
- (7) Gomes, S.; Hagemann, H.; Yvon, K. *J. Alloys Compd.* **2002**, *346*, 206.
- (8) Buchter, F.; Łodziana, Z.; Mauron, P.; Remhof, A.; Friedrichs, O.; Borgschulte, A.; Züttel, A.; Sheptyakov, D.; Strassle, T.; Ramirez-Cuesta, A. J. *Phys. Rev. B* **2008**, *78*, 094302.
- (9) Ikeshoji, T.; Tsuchida, E.; Ikeda, K.; Matsuo, M.; Li, H.-W.; Kawazoe, Y.; Orimo, S.-i. *Appl. Phys. Lett.* **2009**, *95*, 221901.
- (10) Corey, R. L.; Shane, D. T.; Bowman, R. C.; Conradi, M. S. *J. Phys. Chem. C* **2008**, *112*, 18706.
- (11) Remhof, A.; Łodziana, Z.; Martelli, P.; Friedrichs, O.; Züttel, A.; Skripov, A. V.; Embs, J. P.; Strässle, T. *Phys. Rev. B* **2010**, *81*, 214304.
- (12) Skripov, A. V.; Soloninin, A. V.; Filinchuk, Y.; Chernyshov, D. *J. Phys. Chem. C* **2008**, *112*, 18701.
- (13) Tsang, T.; Farrar, T. C. *J. Chem. Phys.* **1969**, *50*, 3498.
- (14) Zarkevich, N. A.; Johnson, D. D. *Phys. Rev. Lett.* **2008**, *100*, 040602.
- (15)
- (16) Copley, J. R. D.; Cook, J. C. *Chem. Phys.* **2003**, *292*, 477.
- (17) Aзуаh, R.; Kneller, L.; Qiu, Y.; Tregenna-Piggott, P. L. W.; Brown, C.; Copley, J.; Dimeo, R. *J. Res. NIST* **2009**, *114*, 341.
- (18) Martelli, P.; Remhof, A.; Borgschulte, A.; Ackermann, R.; Strässle, T.; Embs, J. P.; Ernst, M.; Matsuo, M.; Orimo, S.-I.; Züttel, A. *J. Phys. Chem. A* **2011**, *115*, 5329.
- (19) Sköld, K. *J. Chem. Phys.* **1968**, *49*, 2443.
- (20) Rush, J. J.; Graaf, L. A. d.; Livingston, R. C. *J. Chem. Phys.* **1973**, *58*, 3439.
- (21) Verdal, N.; Hartman, M. R.; Jenkins, T.; DeVries, D. J.; Rush, J. J.; Udovic, T. J. *J. Phys. Chem. C* **2010**, *114*, 10027.
- (22) Bée, M. *Quasielastic Neutron Scattering, Principles and Applications in Solid State Chemistry, Biology and Materials Science*; Adam Hilger: Bristol, 1988.
- (23) Hempelmann, R. *Quasielastic Neutron Scattering and Solid State Diffusion*; Clarendon Press: Oxford, 2000.
- (24) Hagemann, H.; Gomes, S.; Renaudin, G.; Yvon, K. *J. Alloys Compd.* **2004**, *363*, 129.
- (25) Dianoux, A. J.; Volino, F.; Hervet, H. *Mol. Phys.* **1975**, *30*, 1181.
- (26) Yildirim, T.; Gehring, P. M.; Neumann, D. A.; Eaton, P. E.; Emrick, T. *Phys. Rev. B* **1999**, *60*, 314.